

Seismic and non-invasive geophysical surveys for the renovation project of Branciforte Palace in Palermo

Journal:	<i>Archaeological Prospection</i>
Manuscript ID	ARP-20-0010.R1
Wiley - Manuscript type:	Special Issue Article
Date Submitted by the Author:	01-May-2020
Complete List of Authors:	Martorana, Raffaele; University of Palermo, Dipartimento di Scienze della Terra e del Mare - DiSTeM CAPIZZI, PATRIZIA; university of Palermo, Dipartimento di Scienze della Terra e del Mare - DiSTeM
Keywords:	Seismic, Ground Penetrating Radar, Electrical Resistivity Tomography, Ultrasonic Tomography, Infrared Thermography, non-invasive

SCHOLARONE™
Manuscripts

Seismic and non-invasive geophysical surveys for the renovation project of Branciforte Palace in Palermo

Raffaele Martorana¹, Patrizia Capizzi¹

¹Department of Earth and Sea Sciences, University of Palermo, Via Archirafi 20, 90123, Palermo, raffaele.martorana@unipa.it, patrizia.capizzi@unipa.it

Abstract

The renovation project of the historic Branciforte Palace (XVI-XVII century) in Palermo (Italy) was owned by the *Banco di Sicilia Foundation*, with the aim for it to become a multi-purpose center for the promotion of exhibitions and cultural events. In the context of the restoration work, a multi-methodological and non-invasive geophysical study has been carried out. The seismic characterization of the foundation soils was obtained by means of joint interpretations of a Vertical Seismic Profile (VSP), Multichannel Analysis of Surface Waves (MASW) and Horizontal to Vertical Spectral Ratio microtremor analysis (HVSr). The mutually constrained inversion of seismic surveys carried out with different techniques made it possible to obtain a robust interpretation of the foundation soils. Moreover, indoor geophysical surveys have been carried out to identify critical issues in the state of conservation of the floors and wall structures. In particular Ground Penetrating Radar (GPR) profiles and an Electrical Resistivity Tomography (ERT) have been carried out on the floor of the stable of the Palace, to evaluate in detail the state of consolidation of the foundation soil, in correspondence of a double row of marble columns, some of which were affected by differential subsidence. The joint interpretation allowed to generate a 3D model of the foundation's subsoil, highlighting the irregular surface of the foundation rock and to identify the main structural voids responsible for subsidence. Furthermore, some supporting columns have been investigated by means of Ultrasonic Tomography (UST) to verify their state of degradation. Finally, Infrared Thermography (IRT) images of the internal and external walls and of the vaults highlighted differences in the type of masonry and in the state of the plaster.

1. INTRODUCTION

The *Banco di Sicilia Foundation*, as owner of the Branciforte - Raccuja Palace, planned its renovation project and redevelopment to be used for cultural and exhibition spaces. In 2007, the task of drawing up the renovation project was entrusted to the famous designer and architect Gae Aulenti. The restoration and redevelopment work of the building began in October 2008 and ended in May 2012, when the building was reopened to the public (fig. 1). These works had the purpose of creating an important cultural open center for all citizens, with spaces destined to art and culture, through a work of recovery and renovation of the most representative environments of the building (Aulenti G., 2012).

The restorations made it possible to give life back to the Palace, making the whole complex functional and modern, creating environments suitable for different use functions, maintaining the testimonies of the past. One of the main objectives of the project was to restore those important architectural spaces that had lost their original function: the internal road, the main courtyard and the horse stable on the ground floor (Vitaliani, 2012). The internal road was freed from the enclosed spaces that interrupted the perspective cone, so that the main door today leads to a real road, covered only by the central lodge. This latter divides the Palace into two distinct wings, allowing visitors to reach all the different areas of the building: the new exhibition space (located inside the old stable),

1
2
3 the coffee bar, the conference room with about 100 seats, the secondary staircase leading to the
4 ateliers, the internal courtyard that opens up to the offices and all the rooms on the upper floors.

5 Geophysical methods are often applied successfully for cultural heritage purposes (Deiana,
6 Leucci & Martorana, 2018). Particularly, some of them have proved particularly useful for identifying
7 buried archaeological structures, such as ground penetrating radar (GPR) (Leucci et al., 2016),
8 magnetic (Eppelbaum, Khesin, & Itkis, 2001), electrical resistivity tomography (ERT) (Griffiths &
9 Barker, 1994; Fiandaca, Martorana, Messina, & Cosentino, 2010, Casas et al., 2018). Recently in the
10 field of cultural heritage, geophysical techniques are used in an integrated approach aimed at reducing
11 interpretative uncertainties and increasing the robustness of the inverse models (Capizzi et al., 2007;
12 Malfitana et al., 2015, Scudero et al., 2018)). Furthermore, interdisciplinary collaborations, in science
13 and humanities, have proven to be very effective for the investigation of archaeological sites and
14 monumental assets (Bottari et al., 2017; Bottari et al., 2018; De Giorgi & Leucci, 2017; Elfadaly,
15 Attia, Qelichi, Murgante, & Lasaponara, 2018; Malfitana et al., 2018).

16 In cases where one is forced to operate in difficult contexts, where it is important to preserve the
17 integrity of the artistic or architectural artefacts, acquisition techniques have been adapted for indoor
18 (Capizzi, Martorana, Messina, & Cosentino, 2012) and lapideous materials (Cosentino, Capizzi,
19 Fiandaca, Martorana, & Messina, 2009; Cosentino, Capizzi, Martorana, Messina, & Schiavone,
20 2011).

21 To support the renovation work, a geophysical study has been carried out, characterized by a
22 multi-methodological non-invasive approach. Geophysical surveys were carried out in 2010 during
23 the works for the restoration of the Palace, in a phase in which many superfluous additions had already
24 been demolished, for example those that covered the original ground floor and the columns of the
25 horse stable. The geophysical investigation project was developed in consultation with the technicians
26 of the Banco d Sicilia Foundation. including architects, engineers, art historians and archaeologists,
27 who participated in the restoration project.

28 One of the objectives of the study was the seismic characterization of the foundation soils by
29 means of joint interpretations of Vertical Seismic Profiles (VSP), Multichannel Analysis of Surface
30 Waves (MASW) and ambient vibrations measures using Horizontal to Vertical Spectral Ratio
31 (HVSr) analysis (Martorana, Agate, Capizzi, Cavera, & D'Alessandro, 2018a; Martorana et al.,
32 2018b). Another goal was to identify critical issues in the state of consolidation of the large and
33 picturesque environment of the ancient stable of the Palace (Capizzi et al., 2012), in which the roof,
34 is supported by a double row of marble columns which longitudinally divide it into three naves,
35 covered by cross vaults. This was achieved by performing indoor geophysical surveys (fig. 2),
36 including Ground Penetrating Radar (GPR), Infrared Thermography (IRT), Electrical Resistivity
37 Tomography (ERT) and Ultrasonic Tomography (UST).

44 2. HISTORICAL NOTES

45 Compared to the historical urban fabric of the city of Palermo, the Branciforte Palace of the
46 Counts of Raccuja (La Duca, 2012) is located in a particularly interesting and valuable position, in
47 the district formerly known as the "Loggia", in the historic center of Palermo. Thanks to its proximity
48 to the port of La Cala, since medieval times it was the beating heart of trade with the merchant lodges
49 of so-called "foreign nations" of the Genoese, the Pisans and Catalans. The most noble and powerful
50 families of the time operated in this extraordinary location, including the families of the Branciforte,
51 Counts of Raccuja (who later became Princes of Leonforte, Pietraperzia and Butera) and the
52 Lampedusa, who built palaces that were a tangible sign of their power and prestige.

53 According to historical sources, the first nucleus of the Branciforte Palace was built at the end of
54 16th century by Nicolò Placido Branciforte Lanza, Count of Raccuja, as a private residence. The
55 original surface of the Palace occupied about half of the current one, expanding from the
56 aforementioned alley to via Lampedusa. The Palace consisted of a basement, a ground floor with
57 warehouses and stables, a first floor reserved for a mansion and a second floor used as a guesthouse,
58 administration and servants' quarters. Subsequently, in the mid-17th century, Don Giuseppe
59
60

1
2
3 Branciforte decided to expand the Palace: the new building doubled the surface by acquiring an
4 almost quadrangular planimetric conformation, the same today present.

5 The work of expanding and embellishing the Palace continued in the 18th century with the
6 construction of large stables with elegant cross vaults, supported by a double row of Billiemi stone
7 columns. In 1801 the Branciforte family gave the Palace to the Senate of Palermo, which after a
8 radical transformation assigned it to the branch of the Pawnshop of Palermo. The transformation
9 works affected the interior, which changed the original configuration (Spatafora & Volpe, 2012).

10 Subsequently, various events (such as a big fire in 1848, the aerial bombardment of World War
11 II in 1943 and the subsequent reconstruction phases) led the building to take on its current appearance.
12 Since 1997, Branciforte Palace has been owned by the Banco di Sicilia Foundation, which has hosted
13 exhibitions, conferences and other cultural events. Since 2006, the Palazzo has become part of the
14 real estate assets of the Banco di Sicilia Foundation.

15 The architectural redevelopment project involved the installation within the Palace of an
16 exhibition area intended for both temporary and permanent installations (Volpe, 2012), a library, a
17 conference room, representation spaces and ateliers.

21 3. GEOLOGICAL OUTLINES

22 It was possible to reconstruct in a detailed way the stratigraphy of the area thanks to the numerous
23 studies available and also to the recent corings performed for the preliminary studies for the Palermo
24 light Metro system.

25 The succession of Pleistocene marine sediments of the Palermo Plain is widely documented by
26 lithostratigraphic data deriving from geological investigations (Liguori & Cusimano, 1978;
27 Giammarinaro, Spotorno, Sulli, & Catalano, 1999; Contino, Giammarinaro, Vallone, Varsalona, &
28 Zuccarello, 2006; Incarbona et al., 2016). These lithologies are datable from the Middle Pleistocene
29 to the Holocene.

30 The succession includes landfills that cover lithofacies belonging to the calcarenitic-sandy-clay
31 Quaternary complex of the Palermo Plain. In particular, recent and current landfills have thicknesses
32 ranging from a few centimeters to 5-6 m. They include sand and silt with stone elements and
33 fragments of bricks. These lie on the calcarenitic-sandy lithofacies, constituted in this area by
34 bioclastic calcarenites of medium grain, yellowish and whitish color, with a degree of variable
35 cementation, from well cemented and lapidary to weakly cemented, soft and sometimes friable, in
36 layers of centimetric and decimetric thickness alternating with subordinate and thin sandy levels.
37 Calcarenites, often present in lenses, have thicknesses ranging from less than one meter to two meters.
38 Below there are calcarenitic sands of medium-fine grain, sometimes silty or slightly silty, with
39 thicknesses of 20-25 m. Below is the clay-sandy lithofacies, formed in this area by fine gray sands,
40 often silty or weakly silty and/or clayey, with thicknesses between 2 and 5 m. Finally, the Oligo-
41 Miocene quartzarenitic-clayey complex is represented in the area by shales, of gray color, hard and
42 very resistant.

48 4. SEISMIC CHARACTERIZATION OF THE SUBSOIL

49 As part of a general diagnostic framework, some seismic investigations were carried out in order
50 to provide necessary information for the seismic characterization of the building's subsoil, which was
51 essential for the renovation project.

52 A down-hole VSP (Gasperini & Signanini, 1983) was performed in the area of the inner courtyard
53 of the Palazzo Branciforte (fig. 2), using a 30 m deep bore-hole already performed as a stratigraphic
54 coring, whose stratigraphy has been provided. Table 1 summarizes the lithological characteristics
55 obtained by drilling and the average densities used to constrain the results of the VSP.

56 Further seismic investigations were performed to better define the vertical profile of shear waves
57 velocity. A MASW survey and two seismic microtremor HVSR measurements were carried out for
58 the evaluation of resonance frequencies of the foundation soil (fig. 2). Seismic noise measurements
59 were carried out at both ends of the MASW line.

Depth (m)	Lithology	Average density (kg/m ³)
0 – 3.60	Landfill	1750
3.60 – 27.20	Sandy calcarenite	1850
27.20 – 30.00	Silty sands	2000

TABLE 1 Lithological results of the drilling survey and average density used.

4.1. Methods

The VSP technique consists in generating elastic waves through a sledgehammer and measuring the first arrival times of P- and S-waves in a three-component geophone placed inside the hole at equally spaced depth intervals (Gal'perin, 1974). Using different shot directions and analyzing the three components of the motion registered by geophones, it is possible to achieve the travel-times of P- and S-waves traveling from source to geophones and, consequently, to deduce the seismic velocities and the thicknesses of the layers in which they travels, so obtaining information about the subsurface, down to the depths of the well bottom (Wyatt, 1981).

The seismic source used was a sledgehammer weighing 6 kg, dropped from a height of about 2 m. Shear waves were generated with strikes on an iron vertical plate, placed at a distance of one meter from the axis of the hole and cemented to a depth of 50 cm. Pressure waves were generated by strikes on a metal plate resting directly on the ground, at the same distance. The probe in the hole is a three-directional geophone that adheres to tube through a hydraulic jack. The shot records were registered with a sampling interval of 100 μ s and 1024 samples for each track. The stacking procedure (up to seven shots for each recording) was also used to increase the signal/noise ratio. The picking of the arrivals of P and S phases allowed travel times estimates; these, after the correction for the offset (distance between the source and the hole axis) have been used for the calculation of Vp and Vs values as functions of depth and, consequently, of the Poisson ratio.

The MASW method (Park, Miller, & Xia, 1999; Xia, Miller, & Park, 1999) allows to determine a one-dimensional layered model of the S wave velocity. This is achievable thanks to the analysis in the frequency-wave number ($f-k$) domain, where spectral data are examined as a function of the phase velocity and frequency. The identification and the analysis of the dispersion curves related to Rayleigh waves are inverted to obtain information about the S wave velocity.

The MASW seismic survey was carried out using a linear array of vertical 24 geophones, 2 meters spaced and a sledgehammer of 6 kg. The acquisition was carried out with an ABEM Terraloc MK6 high resolution digital seismograph, with measuring time of 1024 ms and a sampling interval of 0.25 ms. The MASW line was located in the street along the main façade of the building. An offset of 2 meters was considered for two shots on the right and the left sides of the array with the aim of verifying the reliability of the seismic velocity spectrum and optimizing and constraining the data inversion. In order to increase the signal/noise ratio, a stacking process was carried out on all acquisitions with a number of stacks equal to 5.

The Horizontal to Vertical Spectral Ratio (HVSr) noise method (Nakamura, 1989; Nakamura, 2000) is widely used to estimate the resonance frequencies of the subsoil (Bonney-Claudet, Cotton, & Bard, 2006). In the hypothesis of stratigraphic amplification, the ratio between the spectrum of the horizontal and the vertical component of the microtremor gives an estimate of the transfer function of surface layers on seismic motion respect to the bedrock. This allows to estimate the amplification frequencies of the seismic motion in order to evaluate the site effects. HVSr is also used to estimate the depth of the seismic bedrock and thickness and seismic velocity of the overburden deposits, by inverting the HVSr curve and obtaining 1D seismic velocity models (Fäh, Kind, & Giardini, 2003; Martorana et al., 2017a; Picotti, Francese, Giorgi, Pettenati, & Carcione, 2017). However, inversion models are affected by large uncertainty, if they are not constrained by detailed stratigraphic information. In spite of this, the uncertainty can be limited using shear wave velocity models obtained

1
2
3 by Multichannel Analysis of Surface Waves (MASW) as constraints (Dal Moro, 2010; Capizzi &
4 Martorana, 2014; Castellaro, 2016; Martorana et al., 2017a; Martorana et al., 2018a).

5 Seismic microtremor was registered by using Tromino datalogger, produced by Micromed. The
6 two recordings lasted 46 minutes each, with a sampling frequency of 64 Hz. The investigations were
7 conducted following the criteria and recommendations of SESAME, "Site EffectS Assessment using
8 Ambient Excitations" protocol (SESAME, 2004).

9 The seismic noise recordings were analyzed with the HVSR method to evaluate any lateral
10 lithological variability and obtain information down to a depth useful for determining the $V_{s,eq}$
11 parameter and for determining the seismic bedrock depth (Cara et al., 2008; Martorana et al., 2017a).

12 Data were processed by the Geopsy software. Each record was divided into 30 second time
13 windows, with the aim of isolating the parts where the signal is most stationary and eliminating
14 transient noises. For each window the three-component amplitude spectrum of the oscillation velocity
15 and the spectral ratio H/V of the horizontal/vertical component was calculated for a frequency range
16 between 0.1 and 64 Hz. Finally, the average H/V curve and the standard deviation were calculated.

17 A check was also carried out on any directivity of the noise source in time and space, which could
18 influence the shape and frequency of the spectral peaks (Mucciarelli, Gallipoli, & Arcieri, 2003). In
19 this sense, if the SESAME criteria are respected, each peak of the curve represents, with good
20 reliability, a local amplification of the ground motion by resonance, caused by the presence of
21 impedance contrasts in the subsoil: the greater the impedance contrast, the greater the expected
22 amplitude of the H/V peak (Castellaro & Mulargia, 2009). This is also called Quasi Transfer Spectrum
23 (Nakamura, 1989; 2000) because it approximates the transfer function of the seismic signal from the
24 bedrock to the surface, and therefore represents a good estimate of the main frequencies of seismic
25 amplification.

30 31 4.2. Results

32 From the VSP data analysis, we found a good agreement with the lithology reported in the
33 stratigraphic columns (Table 2). In fact, V_p values range from 680 m/s and 2240 m/s (fig. 3, a). Data
34 show an almost linear gradient up to a depth of about 3-4 m, in which there is an increase,
35 corresponding to the boundary between the landfill material and sandy, medium-consistent
36 calcarenites. At a depth of about 26 m, V_p value shows a further increase, due to the presence of
37 sandy silts.

38 In a vertical seismic profile the estimates of V_s refer to the vertical propagation direction,
39 perpendicular to the prevailing slope of the layers; generally these estimate, due to the stratification
40 anisotropy, are lower than those in the horizontal direction, evaluable by a seismic refraction profile.
41 V_s values range from 375 m/s to 685 m/s (fig. 3, a). The velocity gradient changes at the transition
42 between the fill material and the sandy calcarenites, at a depth of about 3-4 m and in correspondence
43 with the passage to sandy silts, at a depth of about 26 m. From the knowledge of the values of V_p and
44 V_s it was possible to estimate the trend of the Poisson ratio as a function of depth (fig. 3, b).

45 The VSP enabled also to estimate for the $V_{s,eq}$ parameter a value of 605 m/s, and consequently,
46 to classify the soil type into the category B of the seismic categorization.

47 The MASW data analysis and inversion (fig. 3, c) allowed the definition of a four-layered model
48 of shear wave velocity. Despite the limited investigation depth, less than 30 m, the results obtained
49 are comparable with those of the VSP, giving similar seismic velocity values (table 2).

50 The HVSR resulting curves show a fundamental peak H/V equal to 3.2 at the frequency of 19 Hz
51 and another H/V peak equal to 1.6 at a frequency of 3 Hz (fig. 3, d). The HVSR data have been
52 inverted through the DINVER module of the GEOPSY software (Fäh et al., 2003), considering a five-
53 layered model (fig. 3, e). The HVSR inversions were constrained using the results of the VSP and
54 MASW surveys (table 2), forcing the inverse model parameters within limited intervals centered on
55 those of VSP and MASW models (García-Jerez, Seivane, Navarro, Martínez-Segura, & Piña-Flores,
56 2019). In this way, the search space of the models has been restricted, so as the field of equivalence
57 of the inversion, and the robustness of the interpretative model has been increased (Fig. 3, f).

4.3. Comparison of the inverse seismic models

A comparison between the inversion models obtained from VSP, MASW and HVSR data (fig. 3, e and f), shows that all the models have layers with similar seismic velocities and thicknesses. There is a clear gradient of seismic velocity at the boundary between landfill and sandy calcarenite, at a depth of about 3-4 m and at the passage to the sandy silt, at about 26 m.

Neither the VSP nor the MASW allowed to identify the depth of the seismic bedrock, that is, the geological boundary below which amplification is not expected. On the other hand, HVSR surveys identify a layer of $V_s = 996$ m/s at a depth of about 26 meters. The inverse model relating to the MASW 2 shows a layer having V_s of about 700 m/s at a depth of about 30 m, which is evaluated as a seismic bedrock, in consideration of the other investigations carried out.

The availability of the information obtained from the stratigraphic coring and the VSP made it possible to perform constrained inversions of the data and to obtain robust interpretative models. MASW data were inverted using the depth and velocity obtained from the VSP as a constraint, while HVSR data were inverted using MASW and VSP results, for the most superficial part of the soil. The final interpretative model is therefore characterized by a good surface resolution (within the first 30 meters) obtained thanks to VSP and MASW surveys, and a greater depth of investigation obtained by HVSR.

Table 2 shows the comparison among shear waves velocities and depths of layers identified by the different techniques.

This comparison shows the different degree of resolution of the applied seismic techniques, which however lead to similar interpretation models and is in good agreement with the coring data.

Comparing MASW and VSP models, small differences in the shear wave velocity (V_s) values can be noted, which have to be attributed to anisotropy of the elastic parameters, mainly in the landfill and in the limestone and sands. In fact, the VSP method analyzes subvertical seismic paths, while the MASW method indirectly estimates the values of V_s , from the Rayleigh waves, which propagate in a direction parallel to the horizontal topographic surface. As for the silty sands, the higher value estimated by the HVSR model is most likely caused by the fact that the model gives an average value for a thickness of the silty sands of 56.8 m, with the bed at a depth of 83 m. This is much greater than the investigation depth reached by MASW and VSP (30 m), which give V_s values of 658 m/s and 680 m/s respectively, but investigate only the most superficial part of the silty sands, probably less compacted than the deepest part.

Lithology	VSP		MASW		HVSR	
	V_s (m/s)	depth (m)	V_s (m/s)	depth (m)	V_s (m/s)	depth (m)
Landfill	380	4.0	134	0.5	202	1.0
			321	3.5	282	4.2
Limestone and sands	570	26.0	625	26.0	680	26.2
Silty sands	680	-	658	-	996	83.0
Quartzarenites and shales	-	-	-	-	1637	-

TABLE 2 Comparison among lithology, VSP, MASW and HVSR results.

5. INDOOR GEOPHYSICAL SURVEYS

Indoor geophysical surveys were carried out in support of the renovation project, using integrated non-destructive methods for the reconstruction of a general diagnostic framework, useful to provide information on both the structural characteristics and on the conservation status of the investigated areas. Specifically, the goal was to investigate the structural integrity of the marble columns, the

ground floor and the walls and to evaluate the conditions of general degradation of the basement of the building. The investigations were carried out both with classical and unconventional methods (Cosentino et al., 2009; Cosentino et al., 2011). They included Ground Penetrating Radar (GPR) and Electrical Resistivity Tomography (ERT) surveys on the ground of the stable and three ultrasonic tomographies (UST) on the marble columns. Several thermographic surveys (IRT) were also acquired to assess and document the state of degradation of the plaster of walls and, when possible, to recognize the textures walls.

5.1. Methods

5.1.1. Ground Penetrating Radar

Ground Penetrating Radar (GPR) is a geophysical, non-destructive investigation method that exploits the reflection of electromagnetic impulses when they encounter surfaces characterized by variations in the electromagnetic properties of subsoil (Jol, 2009; Persico, 2014). This method is particularly useful in preliminary explorations of archaeological areas or when in presence of natural and artificial cavities (Goodman & Piro, 2013; Leucci et al., 2016; Casas et al., 2018). A detailed characterization of the subsoil of the stable environment was necessary to understand the reasons that led to a lowering of the base of the columns. For this purpose, GPR surveys have been planned and carried out (Daniels, 2009) using the SIR 3 of the GSSI with 400 and 200 MHz antennas.

GPR surveys were carried out for a total of about 1100 meters, covering most of the stable floor. In fig. 2 the yellow rectangle with dimensions of 38 m x 11 m, encloses the areas investigated by the GPR, even if the coverage of the rectangle was not total, due to logistical difficulties caused by to the renovation works in progress. An acquisition range of 230 ns was used, for the 200 MHz antenna, and of 110 ns, for the 400 MHz antenna. Each GPR profile has been processed and filtered using software ReflexW© to remove coherent and random noise, by applying a static correction, a background removal and the Kirchoff migration.

An average propagation velocity of electromagnetic wave of about 0.07 m/ns was obtained from curvature of the hyperbolas of reflection. From this, a maximum investigation depth was estimated of about 8 meters for the 200 MHz antenna and 3.5 meters for the 400 MHz antenna. In the absence of specific calibrations of the electromagnetic velocity, these average values were imposed on all the profiles carried out. In order to converting time sections in depth sections, the value of the average dielectric constant $\epsilon_r = 15$ was estimated, by means of transparency measurements, where possible. Subsequently GPR profiles were processed for the construction of depth-slices (Conyers, 2006; Masini et al., 2017). These have been calculated using a routine implemented in Matlab.

5.1.2. Electrical Resistivity Tomography

Electrical resistivity surveys are aimed to estimate the electrical resistivity of the subsurface. This method is one of the most used geophysical exploration methods in archeological exploration surveys (Griffiths & Barker, 1994; Tsokas, Tsourlos, Vargemezis, & Pazaras, 2008). The measurements are made by injecting a current into the ground through two current electrodes and measuring the difference in the resulting voltage at two potential electrodes. The basic data from a resistivity survey are the current I injected into the ground and the resulting voltage difference ΔV between the potential electrodes and the positions of the electrodes. From these measures, the apparent resistivity can be evaluated (Spies & Eggers, 1986).

In part of the stable floor a 2D ERT was carried out (fig. 2) by using 91 electrodes aligned with a minimum distance of 0.5 m, for a total length of the profile equal to 45 m.

Drill holes of about 20 mm in diameter and 10 cm in depth were made for each electrode on the stone floor, so as to place the electrodes in direct contact with the ground under the stone floor. In addition, a conductive gel was injected into each drill hole to minimize the contact impedance between the electrode and the ground (Capizzi et al., 2012; Casas et al., 2018). 1475 measurements were performed, using the Linear Grid multielectrode configuration (Martorana, Fiandaca, Casas, &

1
2
3 Cosentino, 2009) in order to minimize the invasivity of the survey. In this way a maximum depth of
4 investigation of about 6 m was reached (Martorana, Capizzi, D'Alessandro, & Luzio, 2017b).
5

6 5.1.3. Ultrasonic Tomography 7

8 At the time of the investigation, the columns of the ground floor had appeared partly or wholly
9 embedded in the more recent masonry structures. The Ultrasonic Tomography (UST) method (Green
10 Jr., 2004) was chosen, among the various technologies to investigate the columns, for its ability to
11 characterize mechanical stress. The main advantages provided by UST, as compared to other non-
12 destructive testing techniques, consist of a high sensitivity provided an acceptable penetration power,
13 allowing to locate relatively small discontinuities (nevertheless larger than the used wavelength).
14

15 The UST surveys were performed on three of these columns, two flanked by retaining walls (fig.
16 8, a), and one free (fig. 8, b), to determine the velocity of the elastic waves in the material and to
17 identify and locate internal anomalies. All the columns are composed by several monolithic blocks
18 of "Billiemi" gray stone, a bluish gray limestone breccia, very hard and compact, widely used as a
19 material for the covering of buildings. Data were acquired using the "transmission" technique, in
20 which, for each source the whole series of receivers is used, positioned with relatively uniform
21 spacing on the outer surface of the object to be investigated. The source is moved, time by time, to
22 each of the receiver positions. In the case of a column a complete 3D UST, however, can be very
23 laborious to be performed. Alternatively, it is possible to carry out a series of parallel 2D UST surveys,
24 by positioning sensors along parallel outer circumferences (2D circular UST) or along vertical
25 opposite directions (2D longitudinal UST). Two of these columns (column 6 and column 8, see fig.
26 4) were investigated for their entire height using 2D circular UST (fig. 8, a). Data has been acquired
27 on the basis of the column and on the rings and on the abacus of the capital. The 3D UST surveys of
28 the columns (for a total height of about 3 meters) were reconstructed by carrying out 26 2D circular
29 UST surveys for column 6 and 25 for column 8, vertically separated from each other by 15 cm. 1196
30 signals for column 6 and 708 signals for column 8 were acquired and processed, for which both the
31 source-receiver distances both traveltimes of p-waves were measured. The column 9 (see fig. 4) has
32 been investigated only in the upper part and in the capital (fig. 8, b). On this column an ultrasonic
33 analysis was performed, through the acquisition of a series of 2D tomographies (Fig. 8, e): six of
34 which carried out along the circumferences of the column and three along the capital, 5 cm spaced,
35 for a total number of 1188 signals.
36

37 The ultrasonic measurements were performed using the TDAS-16 instrumentation produced by
38 Boviari. It is a sixteen-channel device that allows to acquire, thanks to an electronic switch, four
39 channels at a time with a maximum sampling frequency of 1.25 MHz. The system is equipped with
40 receiving and transmitting probes having a central frequency of 55 KHz. The RSG-55 piezoelectric
41 accelerometric receivers have been designed to have a high sensitivity in a frequency range of
42 received signals from 1 KHz to 8 KHz, with a peak at 6KHz (30 V/g), excellent for sounding not
43 particularly coherent materials (like degraded and / or fractured rock in historic buildings,) and a good
44 linear sensitivity for a frequency range of 10 -70 KHz, typical for signals received from concrete or
45 rock samples. The TSG-55 piezoelectric transmitter is of the "sandwich" type with preloaded
46 ceramics and allows the generation of pulses, with a high signal transmission power, and a central
47 frequency of 55 kHz.
48

49 The data acquisition software, managed by a notebook, as well as allowing the setting of the main
50 acquisition parameters (time range between 0.1 ms and 1 s, sampling frequency and gains), allows
51 the control of the quality of the signals and the estimation of the travel times via display of waveforms.
52 Good data quality is ensured by the possibility of adding and stacking hundreds of signals.
53

54 Before processing tomographic data were filtered, eliminating the values considered as outliers
55 after a critical analysis and correction of possible errors (Cosentino & Sanfratello, 2004). A grid of
56 elementary meshes of size 5x5x5 cm was used for the data inversion, performed by the Geotom
57 software.
58
59
60

5.1.4. Infrared Thermography

Infrared thermographic images (IRT) have been carried out in all the facades of the Palace and some of the walls of the inner courtyard, trying to take advantage of the sunlight as much as possible, in order to take pictures during the cooling of the investigated structures (Avdelidis & Moropoulou, 2004; Kylili, Fokaides, Christou, & Kalogirou, 2014). The thermal imager FLIR™ P40 PAL of FLIR System has been used, equipped with a spatial resolution of 1.3 mrad, sensitive to thermal radiation in the band between 7 and 13 μm . The processing of scanned images was performed using the software ThermaCAM Report PRO 7.0 and ThermaCAM Researcher 2.7 (FLIR Systems, 2005). The processing has provided, in addition to normal treatments of noise reduction and of all possible outliers, also the application of techniques emphasizing the differences of temperatures, in order to identify any differences and details in the structure investigated (Grinzato, Vavilov, & Kauppinen, 1998). Data were acquired in the afternoon, after the completion of the solar radiation.

5.2. Results and discussion

3D models obtained from GPR data acquired on the ground of the horse stable were represented in volume rendering and as isosurfaces of normalized amplitude of signal. Sets of data obtained from both antennas (200 MHz and 400Mz) show some anomalies at a depth of about 2 meters, over the entire extension of the investigated area (fig. 4). These anomalies show a limited extension both laterally and in depth and have been interpreted with the presence of cavities and/or inconsistent material. However, some of these have a larger extension, in correspondence with columns 12, 13 and 14 and with columns 10 and 20 and the related rooms (figs. 5, 6). Some direct investigations (exploratory essays) subsequently showed that anomalies are related to zones of structural void (zones 1, 2 and 3 in figs. 5 and 6).

It is also possible to identify a more consistent level at about 3.5 meters deep, probably due to the presence of calcarenite (dashed white line in fig. 5). This depth estimate is quite in agreement with the those obtained from the seismic model and with the coring stratigraphy. However, the depth of this level cannot be considered constant along the whole extension of the stable. Some areas, in fact, show a greater thickness of the landfill and consequently a deepening of the calcarenite layer.

The model obtained by the 400 MHz antenna (fig. 6) also shows the presence of foundations of the perimeter wall which sometimes extend even 2.5 meters towards the inside of the building.

The ERT results (fig. 7) show a surface layer of low resistivity almost continuous (values less than 100 Ωm and thickness less than one meter) which overlooks a highly heterogeneous zone, characterized by wide anomalies with high resistivity ($> 1000 \Omega\text{m}$), until 2.5-3 m of depth. Some resistive anomalies are highlighted at a distance of 10-12 m, 16-18 m and 34-38 m from the starting point A (zones 1, 2, and 3 highlighted in fig. 7), which could be due to the presence of voids or inconsistent filling materials. The positions of these anomalies are in good agreement with the corresponding high reflectivity zones highlighted in the GPR models, thus validating their interpretation. The presence of a conductive anomaly is also showed, at about 12-13 m from A, probably due to the local presence of saturated soils. At depths between 2 and 4 m, the calcarenite roof can be recognized, confirming the results of the GPR. The boundary appears notably wavy and the resistivity of this layer has a heterogeneous distribution with values ranging from about 200 Ωm to 2000 Ωm , probably due to the high variation of the sandy percentage and the degree of fracturing.

Results of the Ultrasonic Tomography carried out on the columns showed velocity values quite homogeneous, with an average velocity of about 6250 m/s of UST1 in column 6 and about 6650 m/s of UST2 in column 8. However, the basement of column 6 shows zones of weakness at relatively low velocity (fig. 8 c). Analyzing in detail the results relating to column 8, on the other hand, at heights from 110 cm to 150 cm from the floor, a near surface zone of weakness is noted, characterized by low velocity (fig. 8, d). Instead, UST3 shows a high velocity zone in the capital of column 9, evidently due to a previous intervention on this column, consisting of an insertion of a stone block in that zone.

Infrared thermographic images (IRT) carried out in the facades of the Palace have not produced very good results. In fact, the perimeter walls of the building, for their azimuthal position and the

1
2
3 presence of other neighboring structures, do not enjoy optimum position nor a good and uniform solar
4 radiation (fig. 9, a), so that the resolving power of the methodology of investigation was rather limited
5 (fig. 9, b). However, positive results were obtained by the indoor thermography of the vaults, which
6 took advantage of the thermal radiation provided by the internal lighting system of the building, thus
7 executing an almost active thermography (fig. 9, c, d). IRT results have revealed the presence of a
8 different thermal behavior of the masonry on the outer perimeter and on the inner courtyard of the
9 building due to different construction methods. On the outer walls, the degradation of the plaster and
10 stone elements is highlighted (fig. 9, a, b). In particular, the plaster, which is not uniformly clinging
11 to the wall surface, shows areas of high humidity and consequently localized degradation, probably
12 due to infiltration of water resulting from rain gutter of the roof, especially in the west wall. In some
13 of the thermographic images of the walls of the inner courtyard the masonry texture is visible, formed
14 by regular ashlars (fig. 9, c, d).
15
16

17 18 **6. CONCLUSIONS**

19 Geophysical surveys have played great importance in the general diagnostic framework of the
20 Branciforte Palace. In particular, the results from the joint analysis of VSP, MASW and HVSR
21 surveys allowed to reconstruct the seismic characteristics of the foundation soil down to depth of 30
22 m, at least, evaluating with good accuracy the trend of pressure and shear wave velocities.
23

24 The mutually constrained inversion of the data obtained from the different seismic techniques,
25 allowed to obtain the seismic characterization of the subsoil, sufficiently detailed in the most
26 superficial part, to evaluate the quality of the foundation soil, but at the same time with the necessary
27 investigation depth for an accurate assessment of the depth of the seismic bedrock, for the purpose of
28 the seismic response.
29

30 The interpretation of GPR and ERT data acquired in the horse stable perfectly agree in locating
31 the area of voids characterized by very high resistivity values, giving information on their spatial
32 arrangement and on the volumes of the anomalous zones. These two methods have jointly detected a
33 large anomalous zone, where the material of the subsoil, at small depth, does not possess
34 characteristics of good consistency, as it has been confirmed by some direct investigations
35 (exploratory excavations). The joint interpretation of these two investigations also made it possible
36 to identify the calcarenite roof, basis of the building's foundations, and to detect its irregularity.
37

38 The ultrasonic tomographies have generally showed a good state of preservation of the columns,
39 highlighting small localized anomalies. Finally, the IRT images showed that the level of plaster
40 degradation was generally wide and widespread, such as the degradation of the visible stone.
41

42 In conclusion, the integrated approach of several geophysical techniques provided detailed
43 information on the structural characteristics and the conservation status of the heritage and of its
44 foundation soils, useful during the restoration phase for the appropriate choices of consolidation and
45 re-architecture of the Palace.
46
47

48 **CONFLICT OF INTEREST**

49 The authors declare that there is no conflict of interest that could be perceived as prejudicing the
50 impartiality of the research reported.
51
52

53 **ORCID**

54 Raffaele Martorana <https://orcid.org/0000-0002-4421-9501>
55 Patrizia Capizzi <https://orcid.org/0000-0002-8750-6105>
56
57
58
59
60

REFERENCES

- Aulenti, G. (2012). Restauro e architettura di Palazzo Branciforte, in G. Puglisi (a cura di), Palazzo Branciforte, Palermo 2012, 42-49.
- Avdelidis, N.P., & Moropoulou, N.P. (2004). Applications of infrared thermography for the investigation of historic structures. *Journal of Cultural Heritage*, **5**, 1, 119-127. <https://doi.org/10.1016/j.culher.2003.07.002>
- Bonnefoy-Claudet, S., Cotton, F., & Bard, P. -. (2006). The nature of noise wavefield and its applications for site effects studies. A literature review. *Earth-Science Reviews*, **79**(3-4), 205-227. doi:10.1016/j.earscirev.2006.07.004
- Bottari, C., Albano, M., Capizzi, P., D'Alessandro, A., Doumaz, F., Martorana, R., Moro, M., & Saroli, M. (2017). Recognition of earthquake-induced damage in the Abakainon necropolis (NE Sicily): results from geomorphological, geophysical and numerical analyses. *Pure and Applied Geophysics*, **175**, 133–148. <https://doi.org/10.1007/s00024-017-1653-4>.
- Bottari, C., Capizzi, P., Cavallaro, D., Coltelli, M., D'Alessandro, A., Lodato, L., Martorana, R., Pisciotta, A., & Scudero, S. (2018). Coseismic damage at an archaeological site in Sicily, Italy: evidence of Roman earthquake surface faulting. *Surveys in Geophysics*, **39**, 6, 1263-1284. <https://doi.org/doi:0.1007/s10712-018-9482-2>.
- Capizzi, P., Cosentino, P.L., Fiandaca, G., Martorana, R., Messina, P., & Vassallo, S. (2007). Geophysical investigations at the Himera archaeological site, northern Sicily. *Near Surface Geophysics*, **5**, 6, 417-426, ISSN 1569-4445. <https://doi.org/10.3997/1873-0604.2007024>
- Capizzi, P., Martorana, R., Messina, P., & Cosentino, P.L. (2012). Geophysical and geotechnical investigations to support the restoration project of the Roman “Villa del Casale”, Piazza Armerina, Sicily, Italy. *Near Surface Geophysics*, **10**, 2, 145-160, ISSN 1569-4445. <https://doi.org/10.3997/1873-0604.2011038>.
- Capizzi, P., & Martorana, R. (2014). Integration of constrained electrical and seismic tomographies to study the landslide affecting the Cathedral of Agrigento. *Journal of Geophysical Engineering*, **11**, 045009. doi:10.1088/1742-2132/11/4/045009.
- Cara, F., Cultrera, G., Azzara, R.M., De Rubeis, V., Di Giulio, G., Giammarinaro, M.S., Tosi, P., Vallone, P., & Rovelli, A. (2008). Microtremor measurements in the city of Palermo, Italy: Analysis of the correlation between local geology and damage. *Bulletin of the Seismological Society of America*, **98**, 3, 1354-1372. <https://doi.org/10.1785/0120060260>
- Casas, P., Cosentino, P.L., Fiandaca, G., Himi, M., Macías, J.M., Martorana, R., Muñoz, A., Rivero, L., Sala, R., & Teixell, I. (2018). Non-invasive geophysical surveys in search of the Roman Temple of Augustus under the Cathedral of Tarragona (Catalonia, Spain): A Case Study. *Surveys in Geophysics*, **39**, 6, 1107-1124. <https://doi.org/10.1007/s10712-018-9470-6>.
- Castellaro, S. (2016). The complementarity of H/V and dispersion curves, *Geophysics*, **81**, 6, T323-T338.
- Castellaro, S., & Mulargia F. (2009). V_{S30} estimates using constrained H/V measurements. *Bulletin of the Seismological Society of America*. **99**, 2 A, 761-773. <https://doi.org/10.1785/0120080179>
- Contino, A., Giammarinaro, M.S., Vallone, P., Varsalona, S., & Zuccarello, A. (2006). Analisi stratigrafico-geotecnica del settore meridionale della città di Palermo finalizzata alla caratterizzazione di fattori di pericolosità sismica in esso presenti. *Bollettino della Società Geologica Italiana*, **125**, 329-343.
- Conyers, L.B. (2006). Ground-penetrating radar for archaeological mapping. In: Wiseman J, El-Baz F (eds) Remote sensing in archaeology. Interdisciplinary contributions to archaeology. Springer, New York.
- Cosentino, P., Capizzi, P., Fiandaca, G., Martorana, R., & Messina, P. (2009). Advances in Microgeophysics for Engineering and Cultural Heritage. *Journal of Earth Science*, **20**, 3, 626-639. <https://doi.org/10.1007/s12583-009-0052-x>
- From Geophysics to Microgeophysics for Engineering and Cultural Heritage. *International Journal of Geophysics*, vol. **2011**, Article ID 428412, 8 pages, ISSN: 1687-885X, EISSN: 16878868.

- 1
2
3 <https://doi.org/10.1155/2011/428412>
- 4 Cosentino, P.L., & Sanfratello, V. (2004). Propagation of errors to two incorrect positions of sources
5 and detectors in wave-field tomography. *Near Surface Geophysics*, **2**, 111-120. ISSN: 1569-4445.
6 <https://doi.org/10.3997/1873-0604.2004008>
- 7 Dal Moro, G. (2010). Insights on surface wave dispersion and HVSR: Joint analysis via Pareto
8 optimality. *Journal of Applied Geophysics*, **72**, 129-140. <https://doi.org/10.1016/j.jappgeo.2010.08.004>
- 9 Daniels, D. (2009) Surface-penetrating radar. The Institution of Electrical Engineers, London.
- 10 De Giorgi, L., & Leucci, G. (2017). The archaeological site of Sagalassos (Turkey): exploring the
11 mysteries of the invisible layers using geophysical methods. *Exploration Geophysics*, **49**, 5, 751-
12 761. <https://doi.org/10.1071/EG16154>.
- 13 Deiana, R., Leucci, G., & Martorana, R. (2018). New perspectives of Geophysics for Archaeology -
14 A Special Issue. *Surveys in Geophysics*, **39**, 6, 1035-1038. <https://doi.org/10.1007/s10712-018-9500-4>
- 15 Elfadaly, A., Attia, W., Qelichi, M.M., Murgante, B., & Lasaponara, R. (2018). Management of
16 Cultural Heritage Sites Using Remote Sensing Indices and Spatial Analysis Techniques. *Surveys
17 in Geophysics*, **39**, 6, 1347-1377. <https://doi.org/10.1007/s10712-018-9489-8>
- 18 Eppelbaum, L. V., Khesin, B. E., & Itkis, S. E., (2001). Prompt magnetic investigations of
19 archaeological remains in areas of infrastructure development: Israeli experience.
20 *Archaeological Prospection*, **8**, 163–185. <https://doi.org/10.1002/arp.167>
- 21 Fähr, D., Kind, F. & Giardini, D. (2003). Inversion of local S wave velocity structures from average
22 H/V ratios, and their use for the estimation of site-effects. *Journal of Seismology*, **7**, 449-67.
23 <https://doi.org/10.1023/B:JOSE.0000005712.86058.42>
- 24 Fiandaca, G., Martorana, R., Messina, P., & Cosentino, P.L. (2010). The MYG methodology to carry
25 out 3D electrical resistivity tomography on media covered by vulnerable surfaces of artistic value.
26 *Il Nuovo Cimento B*, **125**, 5-6, 711-718, ISSN: 2037-4895. <https://doi.org/10.1393/ncb/i2010-10885-3>
- 27 FLIR Systems (2005). ThermaCAM B2: Operator's Manual. Sweden: Flir Systems.
- 28 Gal'perin, E. I. (1974). Vertical seismic profiling. *Tulsa*, SEG.
- 29 García-Jerez, A., Seivane, H., Navarro, M., Martínez-Segura, M., & Piña-Flores, J. (2019). Joint
30 analysis of Rayleigh-wave dispersion curves and diffuse-field HVSR for site characterization:
31 The case of El Ejido town (SE Spain). *Soil Dynamics and Earthquake Engineering*, **121**, 102-
32 120. <https://doi.org/10.1016/j.soildyn.2019.02.023>
- 33 Gasperini, M., & Signanini, P. (1983). The method "down-hole" for the measurement of the seismic
34 waves of land. Technical Review of Friuli Venezia Giulia, No. 4.35 to 37.
- 35 Giammarinaro, M.S., Spotorno, R., Sulli, A., & Catalano, R. (1999). Analisi litostratigrafica del
36 sottosuolo del Centro Storico della città di Palermo finalizzata alla stima della pericolosità
37 sismica dell'area. *Il Naturalista Siciliano*, **24**, 335-337.
- 38 Goodman, D., & Piro, S. (2013). GPR remote sensing in archaeology, geotechnologies and the
39 environment, vol 9. Springer, Berlin
- 40 Green Jr., R.E. (2004). Non-contact ultrasonic techniques. *Ultrasonics*, **42**, 1-9, 9-16.
41 <https://doi.org/10.1016/j.ultras.2004.01.101>
- 42 Griffiths, D. H., & Barker, R. D. (1994), Electrical imaging in archaeology: *Journal of
43 Archaeological Science*, **21**, 153–158. <https://doi.org/10.1006/jasc.1994.1017>
- 44 Grinzato, E, Vavilov, V, & Kauppinen, T. (1998). Quantitative infrared thermography in buildings.
45 *Energy and Buildings*. **29**,1–9. [https://doi.org/10.1016/S0378-7788\(97\)00039-X](https://doi.org/10.1016/S0378-7788(97)00039-X)
- 46 Incarbona, A., Contino, A., Agate, M., Bonomo, S., Calvi, F., Di Stefano, E., Giammarinaro, M.S.,
47 Priulla, A., & Sprovieri, R. (2016). Biostratigraphy, chronostratigraphy and paleoenvironmental
48 reconstruction of the Palermo historical centre Quaternary succession. *Italian Journal of
49 Geosciences*, **135**, 3, 512-525. <https://doi.org/10.3301/IJG.2015.45>
- 50 Jol, H.M. (ed). (2009). Ground Penetrating Radar: Theory and Applications. Elsevier, Amsterdam.
- 51
52
53
54
55
56
57
58
59
60

ISBN 9780444533487

- Kylili, A., Fokaides, P.A., Christou, P., & Kalogirou, S.A. (2014). Infrared thermography (IRT) applications for building diagnostics: A review. *Applied Energy*, **134**, 531-549. <https://doi.org/10.1016/j.apenergy.2014.08.005>
- La Duca, R. (2012). Storia di Palazzo Branciforte, in G. Puglisi (a cura di), Palazzo Branciforte, Palermo 2012, 21-41.
- Leucci, G., De Giorgi, L., Di Giacomo, G., Ditaranto, I., Miccoli, I., & Scardozzi, G. (2016). 3D GPR survey for the archaeological characterization of the ancient Messapian necropolis in Lecce, South Italy. *Journal of Archaeological Science*, **7**, 290–302. <https://doi.org/10.1016/j.jasre.p.2016.05.027>
- Liguori, V., & Cusimano, G. (1978). Il sottosuolo della città di Palermo: caratterizzazione geologica del centro storico. *Bollettino della Società dei Naturalisti in Napoli*, **87**, 289-319. ISSN 0366-2047.
- Malfitana, D., Leucci, G., Fragalà, G., Masini, N., Scardozzi, G., Cacciaguerra, G., Santagati, C., & Shehi, E. (2015). The potential of integrated GPR survey and aerial photographic analysis of historic urban areas: A case study and digital reconstruction of a Late Roman villa in Durrës (Albania). *Journal of Archaeological Science: Reports*, **4**, 276–284. <https://doi.org/10.1016/j.jasrep.2015.09.018>
- Malfitana, D., Leucci, G., Mazzaglia, A., Cacciaguerra, G., De Giorgi, L., Barone, S., Fragalà, G., Pavone, P.D., & Russo, S. (2018). Archaeo-Geophysics Surveys in Pompeii. *Surveys in Geophysics*, **39**, 6, 1219-1238. <https://doi.org/10.1007/s10712-018-9498-7>
- Martorana, R., Agate, M., Capizzi, P., Cavera, F., & D'Alessandro, A. (2018a). Seismo-stratigraphic model of “La Bandita” area (Palermo Plain, Sicily) through HVSR inversion constrained by stratigraphic data. *Italian Journal of Geosciences*, **137**, 1, 73-86. <https://doi.org/10.3301/IJG.2017.18>
- Martorana, R., Capizzi, P., Avellone, G., Siragusa, R., D'Alessandro, A., & Luzio, D. (2017a). Assessment of a geological model by surface wave analyses. *Journal of Geophysics and Engineering*, **14**, 1, 159-172. <https://doi.org/10.1088/1742-2140/14/1/159>
- Martorana, R., Capizzi, P., D'Alessandro, A., & Luzio, D. (2017b). Comparison of different sets of array configurations for multichannel 2D ERT acquisition. *Journal of Applied Geophysics*, **137**, 34–48. <https://doi.org/10.1016/j.jappgeo.2016.12.012>
- Martorana, R., Capizzi, P., D'Alessandro, A., Luzio, D., Di Stefano, P., Renda, P., & Zarcone, G. (2018b). Contribution of HVSR measures for seismic microzonation studies. *Annals of Geophysics*, **61**, 2, SE225. <https://doi.org/10.441/ag-7786>
- Martorana, R., Fiandaca, G., Casas, A., & Cosentino, P.L. (2009). Comparative tests on different multi-electrode arrays using models in near-surface geophysics. *Journal of Geophysics and Engineering*, **6**, 1, 1-20. <https://doi.org/10.1088/1742-2132/6/1/001>
- Masini, N., Capozzoli, L., Chen, P., Chen, F., Romano, G., Lu, P., Tang, P., Sileo, M., Ge, Q., & Lasaponara, R. (2017). Towards an operational use of geophysics for archaeology in Henan (China): methodological approach and results in Kaifeng. *Remote Sensing*, **9**, 8, 809. <https://doi.org/10.3390/rs9080809>
- Mucciarelli, M., Gallipoli, M.R., & Arcieri, M. (2003). The stability of the horizontal-to-vertical spectral ratio of triggered noise and earthquake recordings. *Bulletin of the Seismological Society of America*, **93**, 3, 1407-1412. <https://doi.org/10.1785/0120020213>
- Nakamura, Y. (1989). Method for dynamic characteristics estimation of subsurface using microtremor on the ground surface. Quarterly Report of RTRI (Railway Technical Research Institute) (Japan), **30**, 1, 25-33.
- Nakamura, Y. (2000). Clear identification of fundamental idea of Nakamura's technique and its applications. 12th World Conf. on Earthquake Engineering, 2656.
- Park, R., Miller, D., & Xia, J. (1999). Multichannel analysis of surface waves. *Geophysics*, **64**, 3, 800–808.

- 1
2
3 Persico, R. (2014). Introduction to Ground Penetrating Radar: inverse scattering and data processing.
4 Wiley, Hoboken. ISBN 9781118305003.
- 5 Picotti, S., Francese, R., Giorgi, M., Pettenati, F., & Carcione, J.M. (2017). Estimation of glaciers
6 thicknesses and basal properties using the horizontal-to-vertical component spectral ratio
7 (HVSr) technique from passive seismic data, *Journal of Glaciology*, **63**, 229-248, doi:
8 10.1017/jog.2016.135.
- 9 Scudero, S., Martorana, R., Capizzi, P., Pisciotta, A., D'Alessandro, A., Bottari, C., & Di Stefano, G.
10 (2018). Integrated Geophysical Investigations at the Greek Kamarina Site (Southern Sicily,
11 Italy). *Surveys in Geophysics*, **39**, 6, 1181-1200. <https://doi.org/10.1007/s10712-018-9483-1>
- 12 SESAME (2004). Guidelines for the implementation of the H/V spectral ratio technique on ambient
13 vibrations. Measurements, processing and interpretation. European Commission - Research
14 General Directorate. Project No. EVG1-CT-2000-00026 SESAME. WP12.
- 15 Spatafora, F., & Volpe, G. (2012). Palazzo Branciforte, il volto nuovo di Palermo, *Archeologia viva*,
16 **156**, 22-33, ISSN0392-9485.
- 17 Spies, B. R., & Eggers, D.E. (1986). The use and misuse of apparent resistivity in electromagnetic
18 methods. *Geophysics*, **51**, 7, 1462-1471. <https://doi.org/10.1190/1.1442194>
- 19 Tsokas, G.N., Tsourlos, P.I., Vargemezis, G.N., & Pazaras, N.T. (2011). Using surface and cross-
20 hole resistivity tomography in an urban environment: an example of imaging the foundations of
21 the ancient wall in Thessaloniki, North Greece. *Physics and Chemistry of the Earth*, **36**, 16,
22 1310-1317. <https://doi.org/10.1016/j.pce.2011.03.007>
- 23 Vitaliani, R. (2012). Restauro e riqualificazione di Palazzo Branciforte. Interventi strutturali, in G.
24 Puglisi (a cura di), Palazzo Branciforte, Palermo 2012, 50-60.
- 25 Volpe, G. (2012). La Collezione archeologica della Fondazione Sicilia a Palazzo Branciforte, in G.
26 Puglisi (a cura di), Palazzo Branciforte, Palermo 2012, 68-78.
- 27 Wyatt, K.D. (1981). Synthetic vertical seismic profile. *Geophysics*, **46**, 6, 880-891.
- 28 Xia, J., Miller, R.D., & Park, C.B. (1999). Estimation of near-surface shear-wave velocity by
29 inversion of Rayleigh waves. *Geophysics*, **64**, 691-700.
- 30
31
32
33
34
35
36
37
38
39
40
41
42
43
44
45
46
47
48
49
50
51
52
53
54
55
56
57
58
59
60

1
2
3
4
5
6
7
8
9
10
11
12
13
14
15
16
17
18
19
20
21
22
23
24
25
26
27
28
29
30
31
32
33
34
35
36
37
38
39
40
41
42
43
44
45
46
47
48
49
50
51
52
53
54
55
56
57
58
59
60



FIGURE 1 The Branciforte Palace in Palermo after the renovation project.

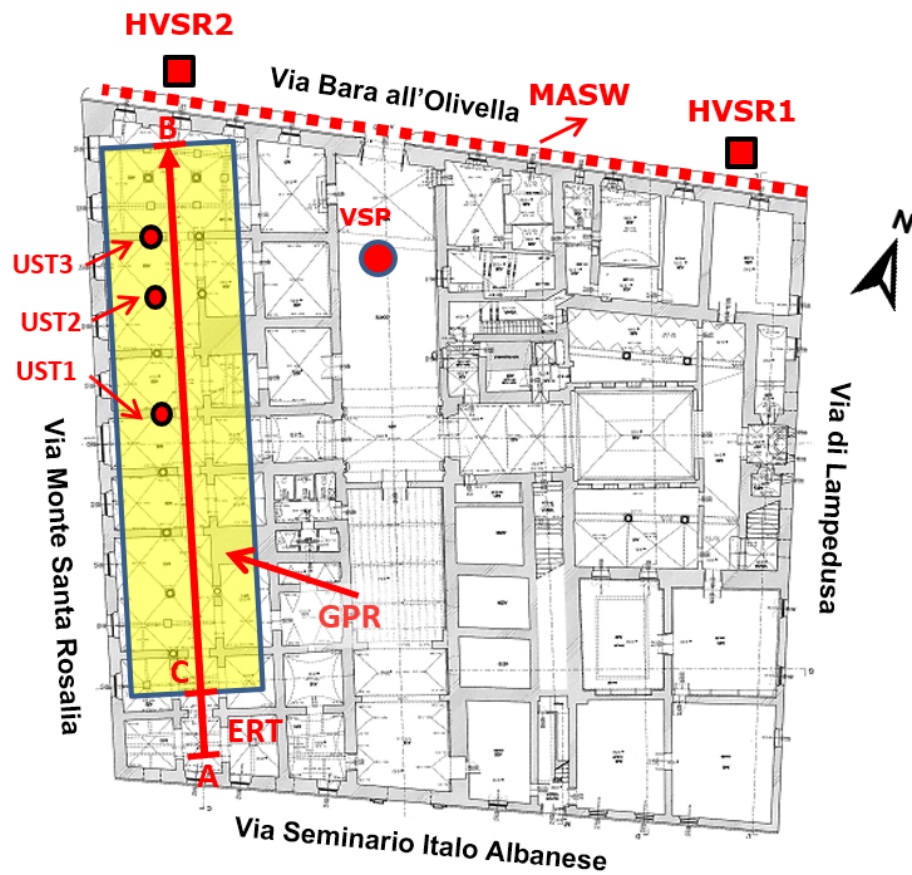


FIGURE 2 Plant of the 1st floor of Branciforte Palace and location of the geophysical surveys. The yellow rectangle encloses the area investigated by GPR surveys, between points C and B. The red straight line indicated the electrical resistivity tomography, between point A and B.

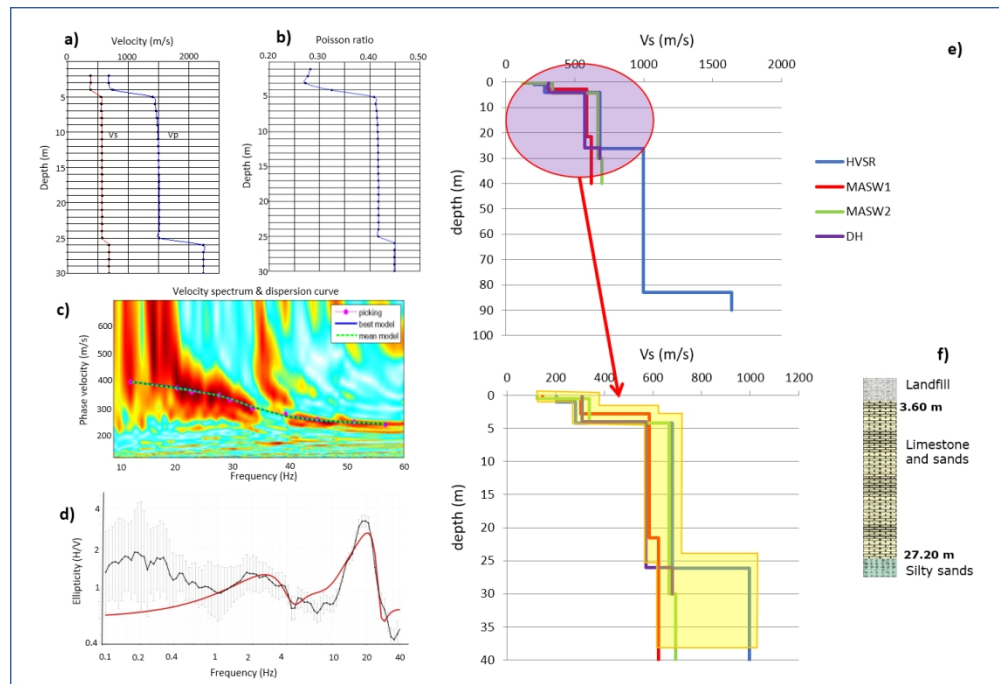
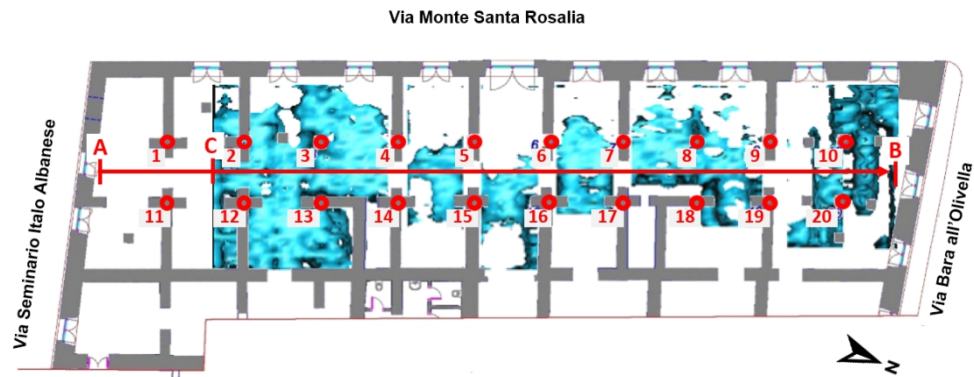


FIGURE 3 Results of the seismic surveys: a) V_p and V_s values estimated by VSP; b) Poisson ratio estimated by VSP; c) Velocity spectrum of the MASW n.1 and overlapped picked and theoretical dispersion curves of the fundamental vibration mode of the Rayleigh waves; d) HVSr curve (measured and theoretical); e) comparison of inverse models; f) details of the inverse models for the near superficial layers compared with lithostratigraphy.



20
21
22
23
24
25
26
27
28
29
30
31
32
33
34
35
36
37
38
39
40
41
42
43
44
45
46
47
48
49
50
51
52
53
54
55
56
57
58
59
60

FIGURE 4 Plant of the stable of Branciforte Palace with referred plain view of the isosurface of normalized amplitude of 0.12 GPR data with 200 MHz antenna. The red circles indicate the columns, the red straight line indicates the ERT profile.

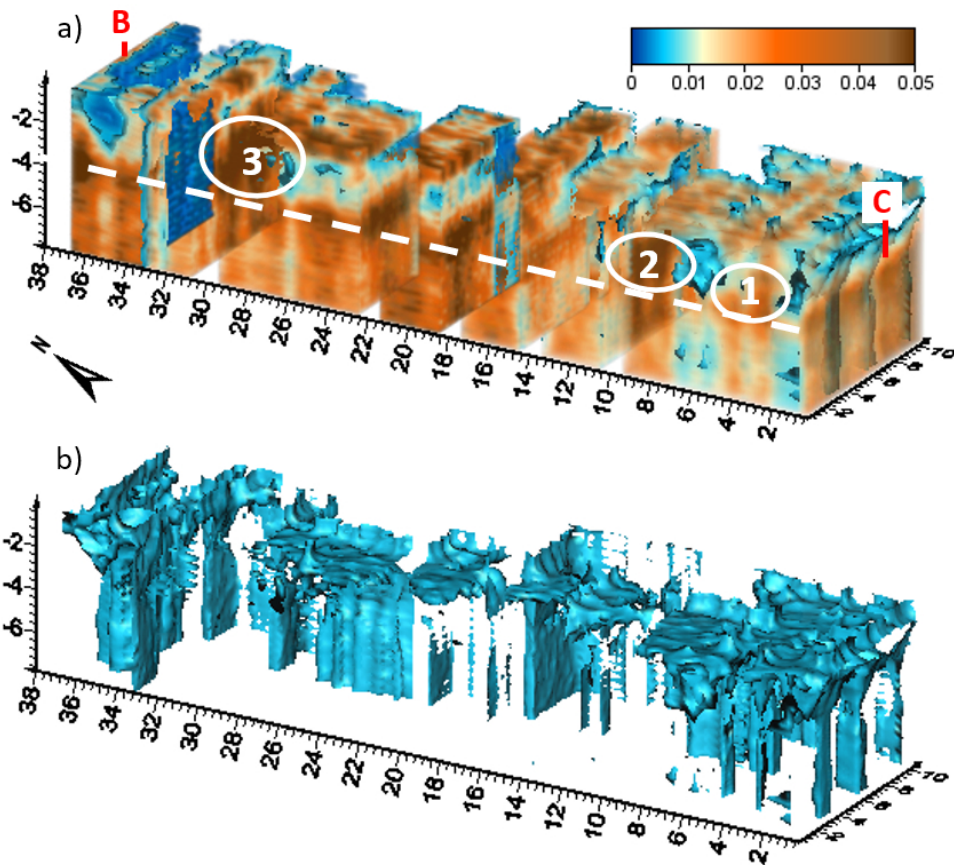


FIGURE 5 3D model of the 200 MHz antenna GPR data: a) volume rendering of the amplitude of GPR signal; the white ellipses indicate the three anomalies discussed in the text. The dashed line indicate the approximated top of the calcarenite layer; b) isosurface of normalized amplitude of 0.06.

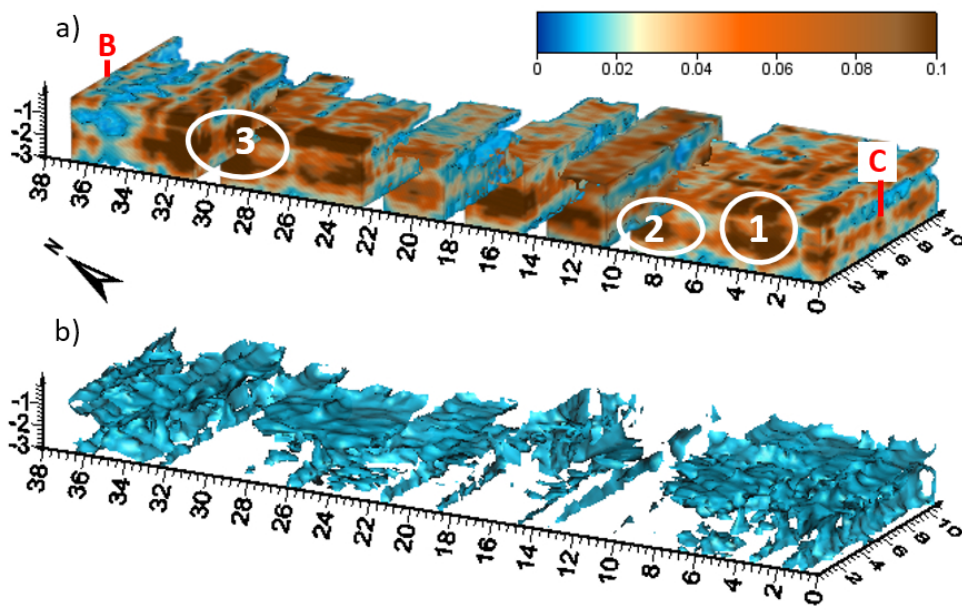


FIGURE 6 3D model of the 400 MHz antenna GPR data: a) volume rendering of the amplitude of GPR signal; the white ellipses indicate the three anomalies discussed in the text. The dashed line indicate the approximated top of the calcarenite layer; b) isosurface of normalized amplitude of 0.06.

1
2
3
4
5
6
7
8
9
10
11
12
13
14
15
16
17
18
19
20
21
22
23
24
25
26
27
28
29
30
31
32
33
34
35
36
37
38
39
40
41
42
43
44
45
46
47
48
49
50
51
52
53
54
55
56
57
58
59
60

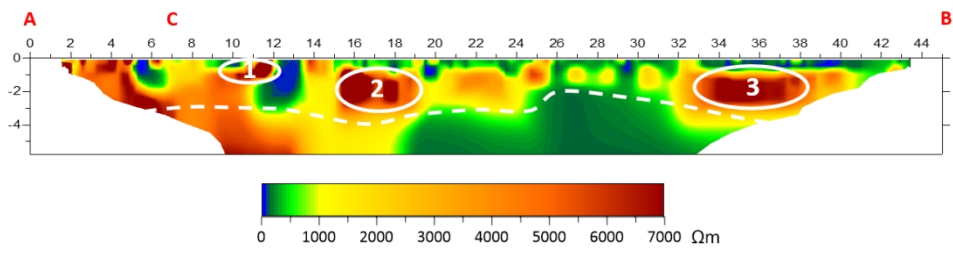


FIGURE 7 Electrical Resistivity Tomography carried out on the stable of Branciforte Palace. The white ellipses indicate the three anomalies discussed in the text. The dashed line indicate the approximated top of the calcarenite layer.

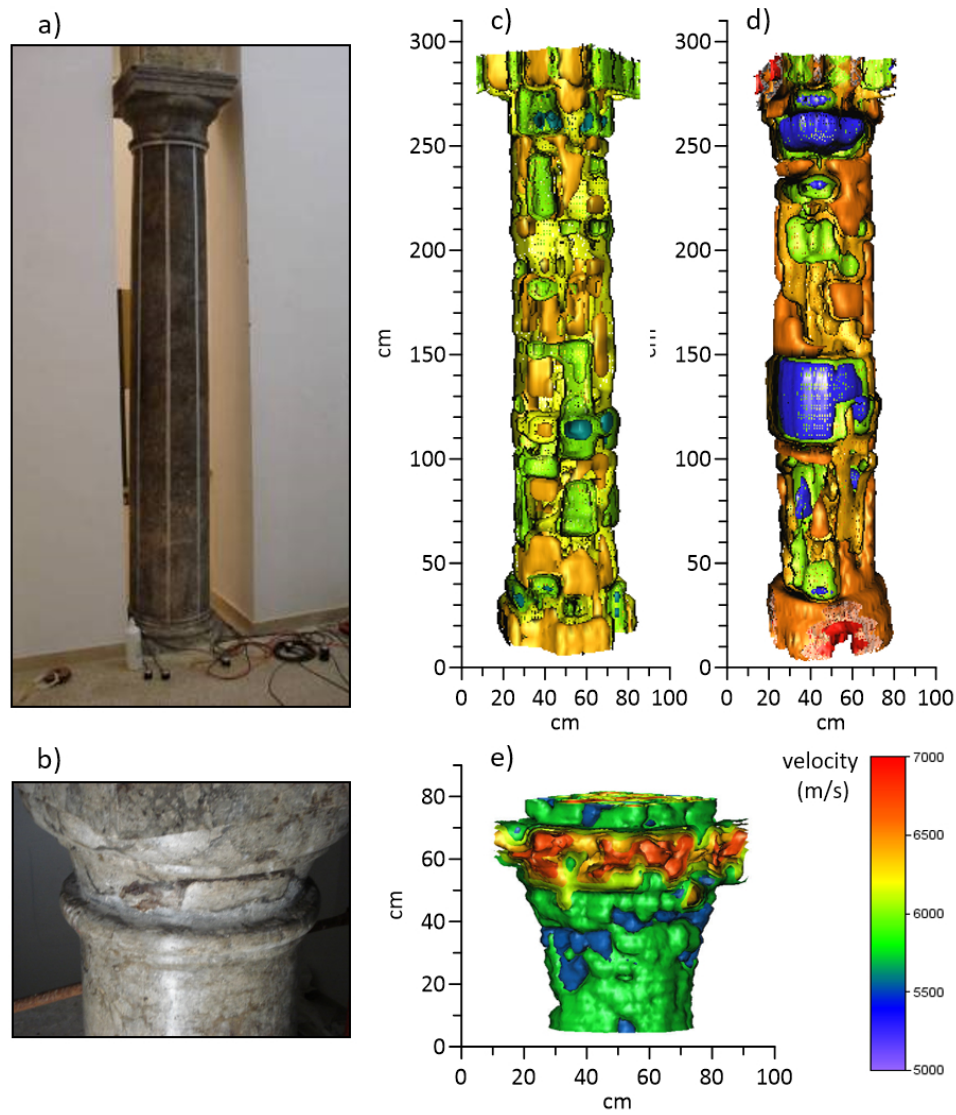


FIGURE 8 Ultrasonic Tomography on the columns of the stable of Branciforte Palace: a) picture of the column 6; b) picture of the capital of column 9; c) UST1 of column 6; d) UST2 of column 8; e) UST3 of the capital of column 9.

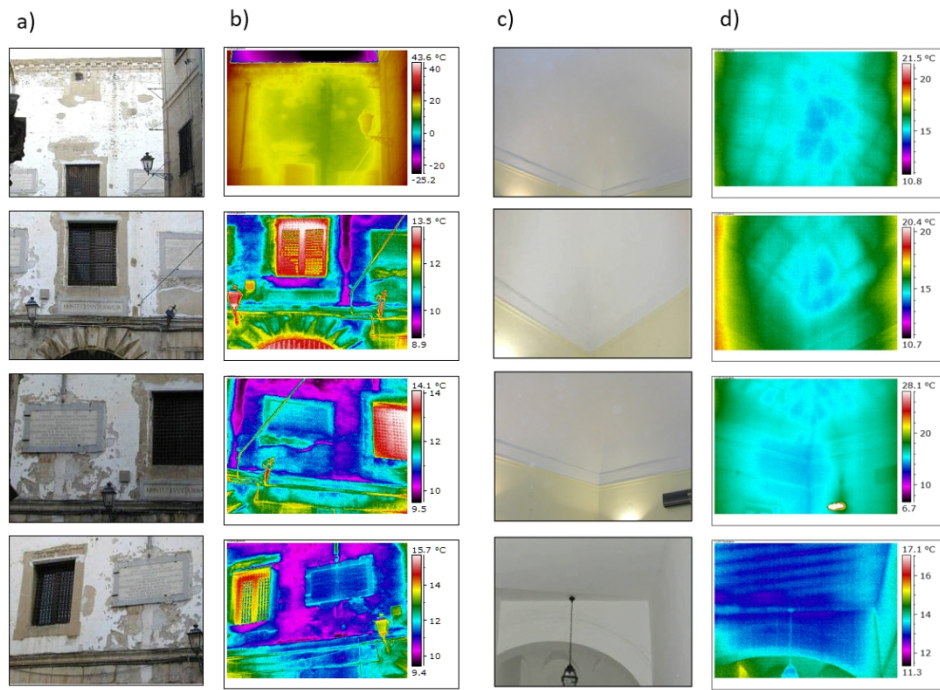


FIGURE 9 Some visible pictures and corresponding IRT images obtained in areas outside (left) and inside (right) the building.